

# Optimal hydrologic regime for regenerating FeIII electron acceptors for iron reduction in upland soils

Salvatore Calabrese<sup>1</sup>, Diego Barcellos<sup>2</sup>, Aaron Thompson<sup>2</sup>, and Amilcare M Porporato<sup>1</sup>

<sup>1</sup>Princeton University

<sup>2</sup>University of Georgia

November 24, 2022

## Abstract

In the predominantly oxic, upland soils, periods of high wetness trigger anaerobic processes such as iron (Fe) reduction within the soil microsites, with implications for organic matter decomposition, the fate of pollutants, and nutrient cycling. In fluctuating O conditions, Fe reduction is maintained by the re-oxidation of ferrous iron, which renews the electron acceptor, Fe, for microbial Fe reduction. To characterize such processes, it is fundamental to relate the redox cycling of iron between the two redox states to the hydro-climatic conditions. Here, we link iron cycling to soil moisture variability through a model of iron-redox dynamics and find the hydrologic regime that maximizes Fe reduction, under non-limiting organic carbon availability. Away from the optimal cycle, the duration of the oxic or the anoxic phase limits the regeneration of Fe or its reduction rate, respectively. We relate the average duration of the oxic and anoxic intervals to the frequency and mean depth of precipitation events that drive the dynamics of soil moisture, effectively linking iron cycling to the hydrologic regime. We then compare a tropical (Luquillo CZO) and a subtropical (Calhoun CZO) forest to provide insights into the soil moisture control on iron-redox dynamics in these ecosystems. The tropical site maintains a high potential for iron reduction throughout the year, due to quick and frequent transitions between oxic and anoxic conditions, whereas the subtropical site is strongly affected by seasonality, which limits iron reduction to winter and early-spring months with higher precipitation and lower evaporative demand.

*O t d e e f e e e t Fe*  
*e e t e t s f ed t d s s*

1

2

3

4

he optimal o ic ano ic c cle or iron e reduction is highlighted

he o ic ano ic c cle and e reduction are related to the soil moisture and rain  
all variabilit

dro climate control on e reduction potential is studied in a tropical and a sub  
tropical orest

in the predominant loessic, upland soils, periods of high wetness trigger anaerobic processes such as iron reductive reduction within the soil microsites, with implications for organic matter decomposition, the fate of pollutants, and nutrient cycling. In fluctuating conditions, reductive reduction is maintained by the re-oxidation of ferrous iron, which renews the electron acceptor, i.e., for microbial reductive reduction. To characterize such processes, it is fundamental to relate the redox cycling of iron between the two redox states to the hydroclimatic conditions. Here, we link iron cycling to soil moisture variability through a model of iron redox dynamics and find the hydrologic regime that maximizes reductive reduction, under non-limiting organic carbon availability. Far from the optimal cycle, the duration of the oxic or the anoxic phase limits the regeneration of iron or its reduction rate, respectively. We relate the average duration of the oxic and anoxic intervals to the frequency and mean depth of precipitation events that drive the dynamics of soil moisture, respectively. Linking iron cycling to the hydrologic regime, we then compare a tropical humid lowland (Congo) and a subtropical (Calhoun Creek) forest to provide insights into the soil moisture control on iron redox dynamics in these ecosystems. The tropical site maintains a high potential for iron reduction throughout the year, due to quick and frequent transitions between oxic and anoxic conditions, whereas the subtropical site is strongly affected by seasonality, which limits iron reduction to winter and early spring months with higher precipitation and lower evaporative demand.

Iron plays a critical role in terrestrial ecosystems, influencing from the carbon cycle to the mobilization of contaminants and the formation of colloidal particles. It is thus important to understand and quantify its biogeochemical cycle in relation to the environmental factors that drive it, for example the oxygen content in the soil pores. Here, we couple its redox cycle, consisting of reductive reduction and subsequent re-oxidation, to the in situ rainfall and soil moisture variability and show that the cycle is faster in a semi-arid climate. These results represent an important step towards predicting the potential for iron redox cycling across different climate and identifying the climatic regions where the biogeochemical cycle may participate more actively in ecosystem functioning.

The iron biogeochemical cycle is an important component of terrestrial ecosystems, where it is implicated in the decomposition of organic matter (Meron et al., 2017; Hattachar et al., 2018; Calabrese et al., 2019; Almeida et al., 2019; Fan et al., 2019; Cheng et al., 2019; A Croi et al., 2019), the formation of colloids (Stucki, 2011; Anderson et al., 2012; Wang et al., 2019) and mobilization of contaminants (Morch et al., 2009; Bishop et al., 2014; Couture et al., 2015; Wu et al., 2016). Predicting the variations in reductive reduction rates as a function of the hydroclimatic requires linking processes from the pedon to the watershed scale, but this has been challenging because of the numerous factors that affect the reductive chemistry.

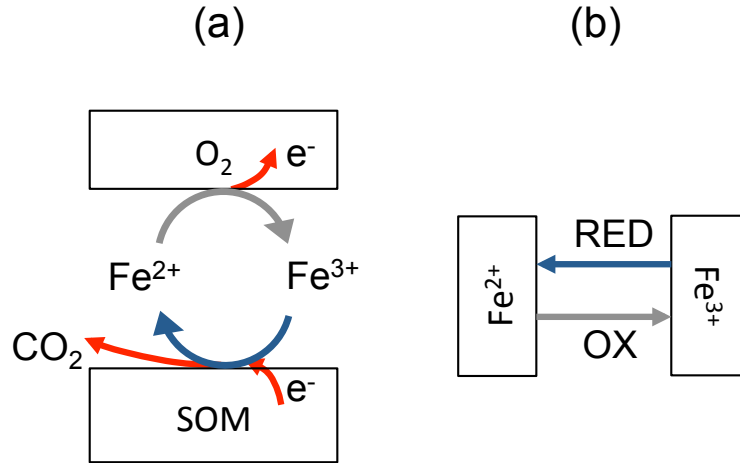
The fundamental constraint on the redox dynamics is the reduction of iron, which has slower kinetics than the oxidation of iron (Lovley, 1991; Finn et al., 2017; Chen et al., 2017). During anoxic conditions, reductive reducing microorganisms rely on the availability of iron oxides as an electron acceptor, reducing it to ferrous iron in order to decompose the organic matter (Lovley, 1991; Roden et al., 1996; Rubin et al., 2010). The rate of reductive reduction thus depends on a suitable organic substrate (Aho et al., 2010; Cappellen, 2011), the activity of reductors, as well as the abundance of iron electron acceptor relative to other more thermodynamically favorable ones (e.g., nitrate, nitrite, nitric oxide, etc.).

The energy yield obtained from oxidizing organic matter coupled to Fe as electron acceptor is lower than the energy yield obtained when coupled to Fe<sup>3+</sup> plus Fe<sup>2+</sup>, Fe reduction is strongly dependent upon the availability of an easily degradable substrate (Aronsson and Cappellen, 2011), whereas those substrates that require more energy to oxidize, i.e., have higher redox potentials, the reduction half-reaction can become thermodynamically unfavorable for microbial Fe reduction. The abundance and activity of Fe reducers is critical for predicting Fe reduction rates. Laboratory and field observations both have shown that Fe reduction is faster when the soil has experienced Fe reduction in the recent past (Mettner et al., 2014; Marcellos, Cline, Thompson, 2018), suggesting increased Fe reducers activity in these conditions. Overall, higher reduction rates are driven mostly by recently oxidized Fe (Eise et al., 2004, 2005; Thompson et al., 2006). The availability of the electron acceptor can in fact be quantified through measurements of short range ordered Fe minerals.

The above arguments suggest that Fe reduction rates are strongly controlled by the characteristics of the soil oxidic and anoxic cycles. In well-aerated soils, oxidic conditions, iron mostly remains in its oxidized state and aerobic respiration is the main mechanism of carbon decomposition, whereas in nearly constantly anoxic environments, such as wetlands and paddy soils, iron mainly persists in its reduced state and other metabolisms typical of low redox potentials may be triggered, i.e., fermentation or methanogenesis (Möller et al., 1993; Radford, 2016). Between these extreme scenarios, a continuous transition between oxidic and anoxic conditions (e.g., wet tropical soils, river banks, fluctuating water tables), which spurs the formation of degradable organic substrates, higher activity of Fe reducers, and the continuous regeneration of Fe<sup>2+</sup>, may favor high rates of iron reduction (Calabrese, Porporato, 2019).

The main environmental factor controlling the transitions between oxidic and anoxic conditions is the soil water content (Goddard et al., 2012; Radford, 2016), as this determines the activity of aerobic bacteria and the fraction of air-filled volume. Experimental studies show that soil moisture may be a proxy for oxygen content, because this remains relatively high (20% or water contents up to the soil field capacity) and then nonlinearly declines to 0 as the soil approaches saturation (Hall et al., 2013; Marcellos, Connell, et al., 2018). Quantification of the state and redox changes of soil iron, necessary for the understanding of the global carbon cycle and related climate dynamics (Colombo et al., 2014; Bertel et al., 2016; Cheng et al., 2019), then needs to be carried out in relation to how hydroclimatic variability can induce changes in soil aeration and redox potential.

To reach this goal, we derive the relationship between the average Fe reduction rate and the length of the exposure to oxidic and anoxic conditions, which is related to the hydrologic regime. We use a mechanistic iron redox model, we explore the interaction between the timescales of the biogeochemistry, i.e., the reaction rates and of the changes in environmental conditions, i.e., oxidic and anoxic cycles and highlight the existence of a maximum average Fe reduction rate at an intermediate anoxic to oxidic intervals ratio. We then relate the oxidic and anoxic cycles to the hydroclimatic fluctuations and link the characteristics of the cycle to the statistical properties of the soil moisture dynamics and precipitation, in terms of its recurrence and mean rainfall depth. This effectively links iron reduction to the in situ hydroclimatic variability, for which measurements are readily obtained through direct or remote sensing techniques. Applying the same approach to soils from a humid tropical forest (Uluwatu C) and a subtropical forest (Calhoun C), we explore the iron redox dynamics in these different ecosystems and discuss its control on the carbon cycle and plant primary productivity.

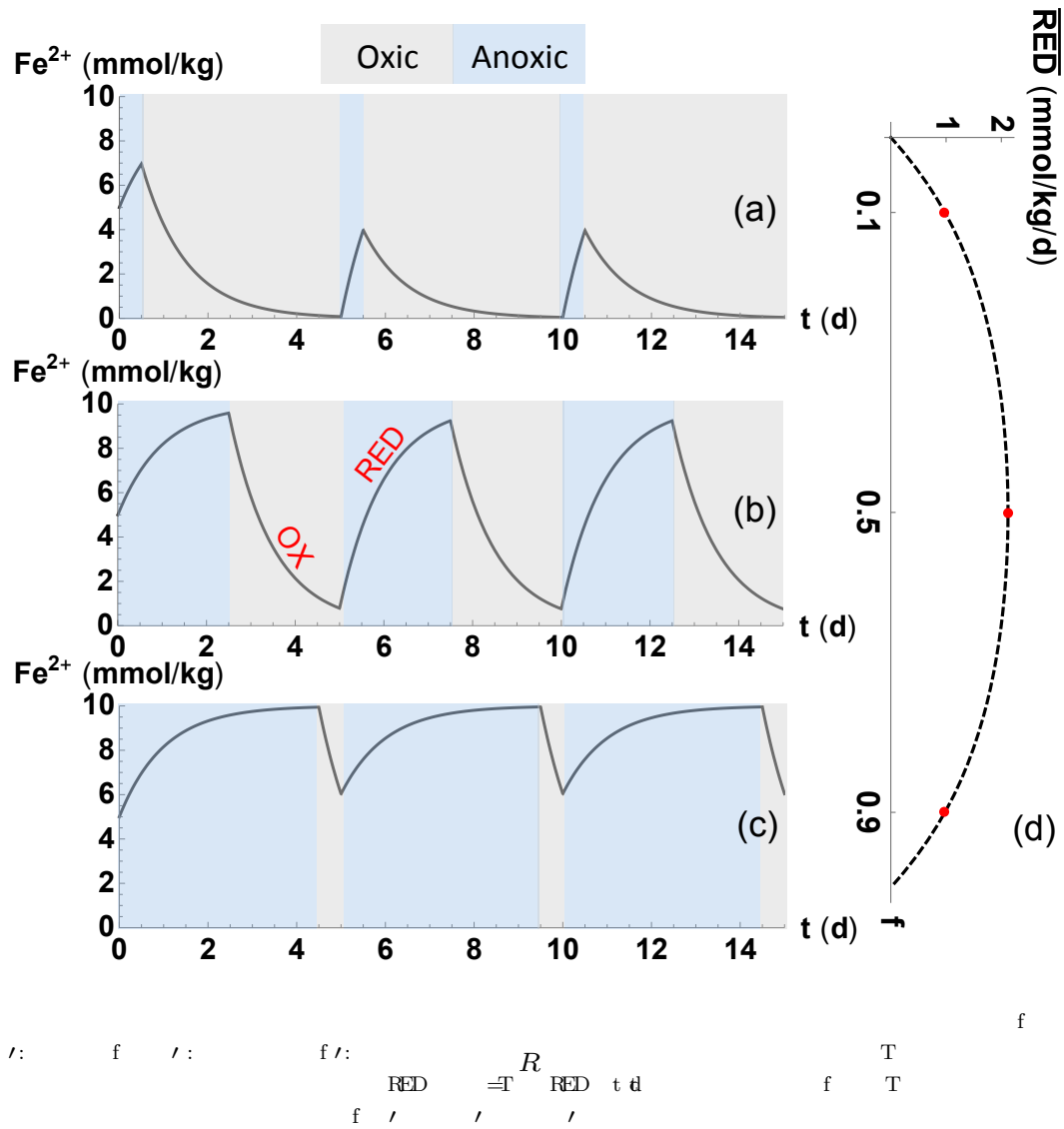


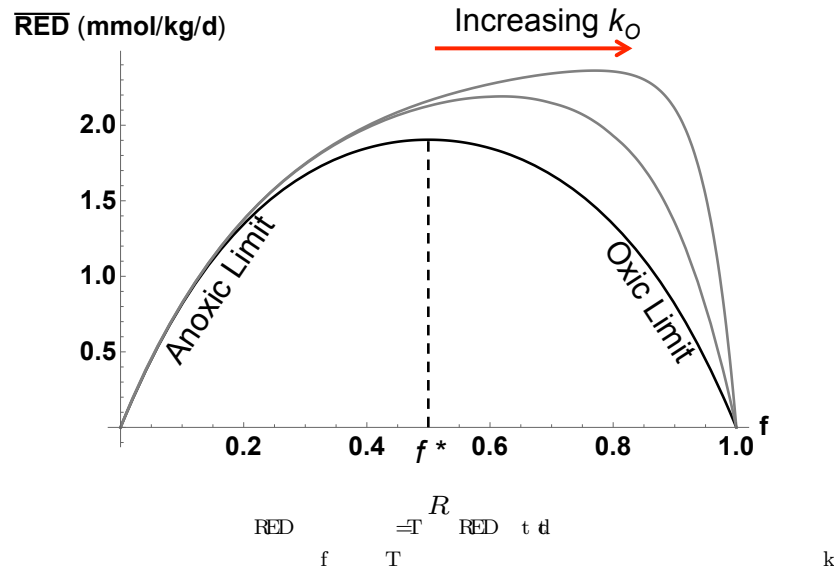
The soil iron cycle, summarized in figure 1 a, has an anoxic phase, in which  $e^-$  is utilized as an electron acceptor to decompose organic matter and an oxic phase, when oxygen oxidizes  $e^-$ , thus regenerating the  $e^-$  pool going back and forth between the two oxidation states, iron operates as an electron carrier between the soil organic matter and the atmospheric oxygen figure 1 a, so that the decomposition depends on the rate at which electrons can be transported from the organic matter to oxygen. Decomposition by iron reduction in fact needs a continuous supply of iron, which after having been reduced to  $e^-$  during an anoxic phase needs to be regenerated, i.e., re-oxidized during the subsequent oxic phase. It is thus clear that the hydroclimate generating the oxic and anoxic cycles exerts a major control on the rate of iron cycling.

Consider the top soil layer containing organic matter and refer to the total iron content in the oxidized and reduced states as  $E^+$  and  $E^-$ , respectively. The total content of reducible iron is constant and equal to  $E^+ + E^-$ . Since our focus is on the maximum rates, we assume that the availability of the organic substrate and microbes does not limit the reactions, so that the regeneration of the electron acceptor and presence/absence of anoxic conditions limit the reaction. The hydrologic cycle will thus govern the reaction rates in this frame or the soil is subject to an oxic and anoxic cycle of duration  $T$  that begins with the anoxic phase of duration  $fT$  figure 2, whereas the oxic phase lasts for  $(1-f)T$ ,  $f$  being the anoxic fraction. During the anoxic phase, only iron reduction occurs; no oxidation allowed, with a consequent increase of  $E^-$ . During the oxic phase, iron reduction stops and  $E^-$  is oxidized to  $E^+$  figure 1 b. Such dynamics are described by the following mass balance equation,

$$\frac{dE^-}{dt} = B - E^- \quad (1)$$

here  $B = k^+ E^+ - E^-$  and  $E^- = k^- E^-$ ,  $k^+$  and  $k^-$  being the reduction and oxidation rate constants, respectively. Note that these expressions do not contain a dependence on the amount of substrate and microbial activity, as we are focusing exclusively on the hydrologic regime. However, the rate constants do explicitly depend on the time,  $t$ , in that during the anoxic phase  $k^- = 0$ , while during the oxic phase  $k^+$





0 Solving equation 1 for sufficiently long time such that the initial condition has no longer influence, the stationary solution for a given oxic and anoxic cycle shown in figure 2 a is given by an exponential decay during the oxic phase,

$$E(t) = E_0 e^{-\lambda t} \quad (2)$$

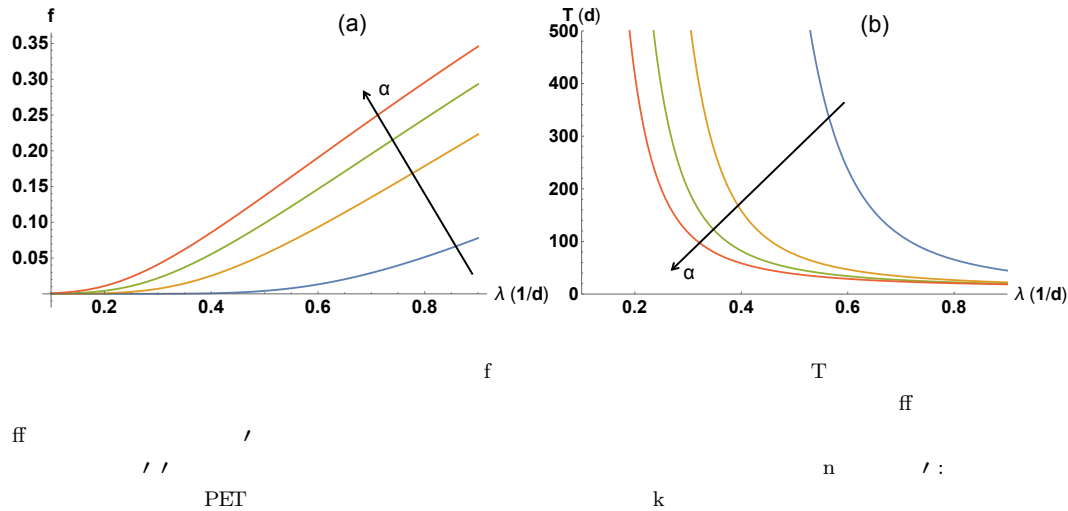
here  $E$  is the iron content at the end of the preceding anoxic phase and  $t$  is the time elapsed since the beginning of the oxic phase. In the contrary, during the anoxic phase  $E$  increases, approaching exponentially  $E^0$ ,

$$E(t) = E^0 (1 - e^{-\lambda t}) \quad (3)$$

$E^0$  being the iron content at the end of the preceding oxic phase and  $t$  the time elapsed since the beginning of the anoxic phase.

In an extreme scenario, in which conditions are set to be all anoxic ( $f = 0$ ), figure 2, iron content persists in its oxidized state ( $E(t) = 0$ ), and the average reduction rate, which can be defined as  $\overline{R} = \frac{1}{T} \int_0^T R(t) dt$ , goes to zero. On the other hand, for a scenario of constant anoxic conditions ( $f = 1$ ), figure 2, iron persists in its reduced state,  $E(t) = E^0$ , and again the reduction rate  $\overline{R} = 0$ . This argument suggests that a maximum reduction rate  $\overline{R}$  exists at an intermediate value of  $f$ ,  $f^*$ . Solving equation 1 for different values of  $f$ , the different trajectories are shown in figure 2, and computing the average reduction rate per cycle, see figure 2 d, illustrates the anoxic-oxic cycle for which the  $\overline{R}$  is maximum.

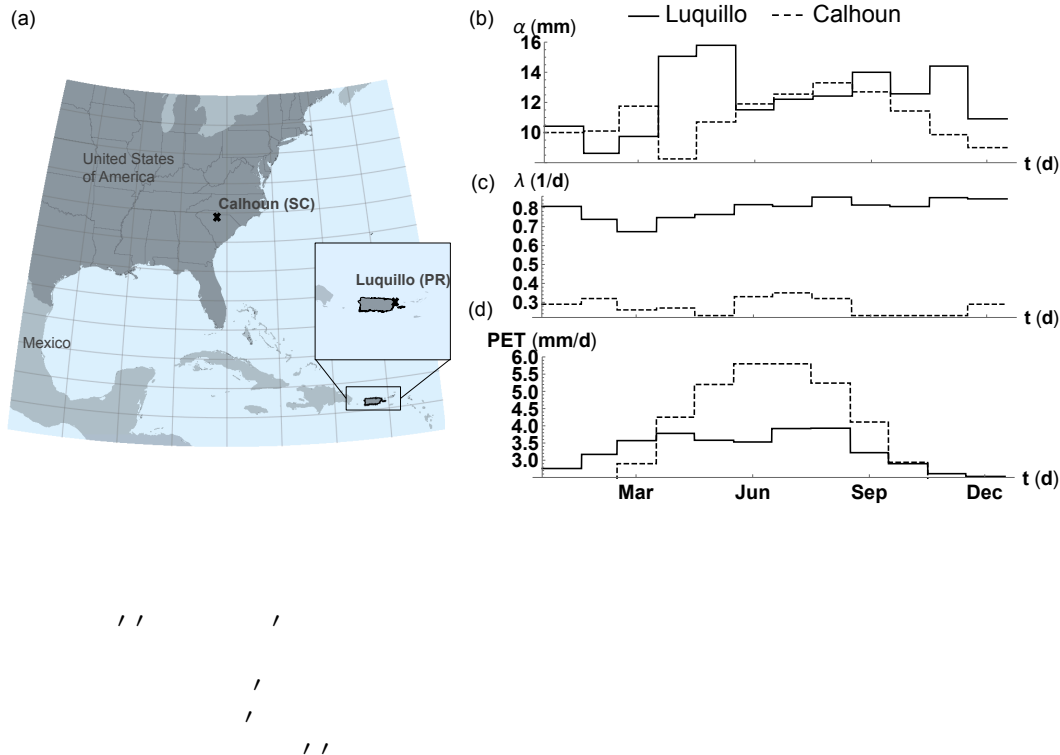
The optimal  $f$  at which the maximum  $\overline{R}$  is achieved depends on the reaction rate constants,  $k$  and  $k^*$ . For simplicity, figure 2 demonstrates that, in the hypothetical condition in which  $k = k^*$ , the resulting  $f^* = 0.5$ . For higher  $k$  or  $k^*$ , shorter anoxic or oxic phases are needed to reduce or oxidize the same amount of iron, respectively. As the ratio of anoxic-oxic time moves away from the optimal  $f$ , the oxic and anoxic cycles favoring either the reduction ( $f < f^*$ ) or the oxidation ( $f > f^*$ ), leading to an inhibition of recycling. When  $f \rightarrow 0$ , the iron redox cycle is limited by the regeneration of the electron acceptor, as essentially there is not enough time to oxidize enough sufficient iron to use in the following anoxic phase. In the contrary, when  $f \rightarrow 1$ , the iron redox cycle is limited by the reduction, such that the anoxic phase is too short to reduce substantial amounts of iron (figure 3).



Under field conditions, the re-entrance and depth of the rainfall events, evapotranspiration from soil and plants, and soil properties altogether determine the evolution of the soil water and oxygen content, causing the soil to undergo transitions between oxic and anoxic conditions. Since oxygen content exhibits a first dependence on soil moisture (Allard et al., 2013; Calabrese et al., 2019), the average duration of the oxic and anoxic phases, for a given hydro-climate, can be obtained by analyzing the specific time series of soil moisture. Using the soil moisture thresholds above which soil conditions can be considered anoxic, there are enough anoxic soil microsites to activate anaerobic processes, the average time spent in oxic conditions can then be calculated as the average time of each excursion below the thresholds. The average time of each excursion above will be, the average duration of a oxic anoxic cycle  $T$ , and in turn the anoxic fraction of time  $f = 1 - T / T_{\text{cycle}}$ .

We show the relationship between the anoxic fraction  $f$ , cycle length  $T$  and the re-entrance and mean depth of precipitation  $\lambda$  and  $\alpha$ , respectively, in Figure 4. The curves are drawn for constant soil properties typical of a silt-clay-loam and potential evapotranspiration  $PET = 4 \text{ mm d}^{-1}$  using a stochastic water balance that provides the statistical properties of soil moisture based on rainfall statistics (Gao et al., 2001; see Appendix). Because of the high water losses at soil moisture above field capacity, the fraction of time spent in anoxic conditions is generally lower than the one spent in oxic conditions, such that the values of  $f$  are below 0.5. Figure 4 shows that, as expected, soils are in anoxic conditions on average longer. Higher values of  $f$  or high rainfall re-entrances accompanied by high average rainfall depths. On the contrary, the whole duration of the cycle,  $T$ , decreases with  $\lambda$  as the excursion from oxic to anoxic is more likely to occur. For the realistic range of mean rainfall depth  $\lambda$  and re-entrance  $\alpha$  explored, the length of the full anoxic and oxic cycle  $T$  decreases with  $\alpha$ , again because it becomes more likely that the soil moisture thresholds is crossed. However, for very high mean rainfall depth  $\alpha$  and re-entrance  $\lambda$  the trend in Figure 4 may be inverted as the soil switches to wet conditions that are in anoxic conditions for most of the time.





The comprehensive hydrological and biogeochemical observations at the tropical forest in Luquillo Puerto Rico and at the subtropical forest in Calhoun South Carolina, which are part of the Critical Zone research network sponsored by the National Science Foundation, allow us to readily apply the above framework to compare the soil iron dynamics and the potential for iron reduction in these different environments. In Luquillo, the focus on the island watershed, where many ecocliming studies have been performed at that site, the mean annual precipitation is about 3500 mm and the vegetation belongs to the bonuco forest type (Scatena, 1989). Soils are predominantly Ultisols, formed from volcanic parent material, and belong to the silt-clay loam textural class. Calhoun has mean annual precipitation of approximately 1250 mm and vegetation includes mixed hardwood and pine trees. Here soils are also predominantly Ultisols, formed from a granite gneiss bedrock, and belong to the silt loam textural class (Schmidt et al., 2001).

Monthly averaged mean depth and frequency of precipitation as well as potential evapotranspiration for the two sites are illustrated in Figure 5. While Luquillo has a humid tropical climate with only a mild seasonality (slightly reduced rainfall in the winter season), Calhoun has a subtropical climate with marked seasonality in both precipitation and evaporative demand, June and July being the wettest months with also a peak in potential evapotranspiration. Geochemical analyses showed that Luquillo and Calhoun soils have approximately 150 and 45 mmol, respectively, of short-range ordered or local crystalline phases per kilogram of soil (Jinn et al., 2017; Arcellós, C. L., Thompson, 2018; Arcellós, 2018). Soil incubation experiments with soil samples from both sites amended with substrate and microbes revealed that reduction rate constants are of the

Figure 6. (a) Temporal evolution of soil moisture, simulated by means of the stochastic model in (Laio et al., 2001), in Luquillo (blue line) and Calhoun (green line) over the course of a year. Soils are silty clay loams and silty loams in Luquillo and Calhoun, respectively, with porosity of 0.48. Soil hydrologic properties for the simulation of the soil moisture dynamics from Fernandez-Illescas et al. (2001). Soils are considered to have sufficient anoxic microsites to support Fe reduction for soil moisture levels above  $\theta = 0.85$  in Luquillo and  $\theta_s = 0.75$  in Calhoun. (b) Anoxic fraction of the cycle,  $f$ , and (c) duration of the cycle,  $T$ , for each month computed by means of equations (??) and (??) in the Appendix. (d) Temporal evolution of  $\text{Fe}^{II}$  in Luquillo (gray line) and Calhoun (red line) over the course of a year, simulated through equation (1). The reduction and oxidation rate constants are  $k_R = 0.1$  and  $k_O = 10$  mmol/kg/d, respectively.

order of  $10^{-1} \text{ d}^{-1}$ , while the oxidation rate constants at 21%  $\text{O}_2$  are of the order of  $10 \text{ d}^{-1}$  (Chen & Thompson, 2017; Ginn et al., 2017).

## 4.2 Oxidic/anoxic cycles and iron reduction

To calculate the temporal dynamics of potential iron reduction (when limited only by the hydrologic regime), we solved equation (1) coupled to a soil water balance that generates a time series of soil moisture levels based on the frequency and mean depth of precipitation events (Figure 6). For Luquillo these rainfall statistics are available in Heartsill-Scalley et al. (2007) and Calabrese and Porporato (2019), while in Calhoun they were obtained combining multiple sources ("<http://criticalzone.org/calhoun/data/datasets/>" and "<https://www.usclimatedata.com/climate/south-carolina/united-states/3210>"). The average anoxic fraction  $f$  and cycle length  $T$  of the oxic/anoxic cycles are then computed for each month from the probability density function of soil moisture (see Appendix A). Note that for each month the parameters  $f$  and  $T$  are computed assuming stationary climatic conditions. For each month their values thus correspond to oxic/anoxic cycles that would occur if the climatic conditions were stationary and typical of that specific month. As a consequence, it can happen that the value of  $T$  is greater than the duration of the month, e.g.,  $T = 80$  days in Calhoun in September. Of course, these large values of  $T$  for a particular month only indicate that it is very unlikely to observe full redox cycles (an Fe oxidation event and an Fe reduction event) in that given month, typically because soil moisture remains below the threshold set.

In Luquillo, the soil moisture frequently crosses the threshold, generating redox cycles of only a few days (2-3 days) throughout the year (Figure 6(a) and (c)). Similarly, the calculated anoxic fraction  $f$  remains practically constant during the year and approximately equal to 0.3 (Figure 6(b)). The mild seasonality here is almost not visible in the

- minerals [10.1029/2018JG002401](#), **3**, 186–203
- onan, [10.1029/2018JG002401](#), 2008 Forests and climate change: forcings, feedbacks, and the climate benefits of forests [10.1029/2018JG002401](#), **8**, 5882, 1444–1449
- orch, [10.1029/2018JG002401](#), retschmar, [10.1029/2018JG002401](#), appeler, [10.1029/2018JG002401](#), Cappellen, [10.1029/2018JG002401](#), inderogel, [10.1029/2018JG002401](#), oegelin, [10.1029/2018JG002401](#), Campbell, [10.1029/2018JG002401](#), 2009 Biogeochemical redox processes and their impact on contaminant dynamics [10.1029/2018JG002401](#), **4**, 1, 15–23
- rad, [10.1029/2018JG002401](#), C, [10.1029/2018JG002401](#), eil, [10.1029/2018JG002401](#), 2016 [10.1029/2018JG002401](#) earson uettner, S, [10.1029/2018JG002401](#), rammer, [10.1029/2018JG002401](#), Chadwick, [10.1029/2018JG002401](#), Thompson, [10.1029/2018JG002401](#), 2014 Mobilization of colloidal carbon during iron reduction in basaltic soils [10.1029/2018JG002401](#), **2**, 139–145
- Calabrese, S, [10.1029/2018JG002401](#),orporato, [10.1029/2018JG002401](#), 2019 Impact of ecophysiological adjustments on iron redox cycling [10.1029/2018JG002401](#)
- Chacon, [10.1029/2018JG002401](#), Silver, [10.1029/2018JG002401](#),ubins, [10.1029/2018JG002401](#), Cusack, [10.1029/2018JG002401](#), 2006 Iron reduction and soil phosphorus solubilization in humid tropical forest soils: the roles of labile carbon pools and an electron shuttle compound [10.1029/2018JG002401](#), **8**, 1, 67–84
- Chen, C, [10.1029/2018JG002401](#), Thompson, [10.1029/2018JG002401](#), 2017 Ferrous iron oxidation under varying pO<sub>2</sub> levels: the effect of microbial iron oxide minerals and organic matter [10.1029/2018JG002401](#), **3**, 2, 597–606
- Colombo, C, [10.1029/2018JG002401](#),alumbo, [10.1029/2018JG002401](#), e, [10.1029/2018JG002401](#),inton, [10.1029/2018JG002401](#), Cesco, S, 2014 Evidence on iron availability in soil: interaction of the minerals, plants, and microbes [10.1029/2018JG002401](#), **4**, 3, 538–548
- Couture, [10.1029/2018JG002401](#), Charlet, [10.1029/2018JG002401](#),arellova, [10.1029/2018JG002401](#),ade, [10.1029/2018JG002401](#), arsons, C, 2015 Iron-mobilization of contaminants in soils during redox oscillations [10.1029/2018JG002401](#), **4**, 5, 3015–3023
- ubins, [10.1029/2018JG002401](#), Silver, [10.1029/2018JG002401](#),irestone, [10.1029/2018JG002401](#), 2010 Tropical forest soil microbial communities couple iron and carbon biogeochemistry [10.1029/2018JG002401](#), **9**, 9, 2604–2612
- [10.1029/2018JG002401](#), 2015 Status of the world's soil resources – main report [10.1029/2018JG002401](#), **0**
- ernande-llecas, C, [10.1029/2018JG002401](#),orporato, [10.1029/2018JG002401](#), aio, [10.1029/2018JG002401](#), odrigue-turbe, [10.1029/2018JG002401](#), 2001 The ecophysiological role of soil texture in a water-limited ecosystem [10.1029/2018JG002401](#), **3**, 12, 2863–2872
- o, C, [10.1029/2018JG002401](#),Chane, [10.1029/2018JG002401](#), t, [10.1029/2018JG002401](#), hite, [10.1029/2018JG002401](#), 1978 The physiology of metal toxicity in plants [10.1029/2018JG002401](#), **9**, 1, 511–566
- inn, [10.1029/2018JG002401](#), eile, C, [10.1029/2018JG002401](#), ilmoth, [10.1029/2018JG002401](#), ang, [10.1029/2018JG002401](#), Thompson, [10.1029/2018JG002401](#), 2017 Rapid iron reduction rates are stimulated by high amplitude redox adjustments in a tropical forest soil [10.1029/2018JG002401](#), **5**, 6, 3250–3259
- ross, [10.1029/2018JG002401](#), ettledge, [10.1029/2018JG002401](#), Silver, [10.1029/2018JG002401](#), 2018 Soil oxygen limits microbial phosphorus utilization in humid tropical forest soils [10.1029/2018JG002401](#), **2**, 4, 65
- uerinot, [10.1029/2018JG002401](#), i, [10.1029/2018JG002401](#), 1994 Iron: nutritious, noxious, and not readily available [10.1029/2018JG002401](#), **4**, 3, 815
- all, S, [10.1029/2018JG002401](#), c o ell, [10.1029/2018JG002401](#), Silver, [10.1029/2018JG002401](#), 2013 When it gets better: decoupling of moisture, redox biogeochemistry, and greenhouse gas fluxes in a humid tropical forest soil [10.1029/2018JG002401](#), **6**, 4, 576–589
- an, [10.1029/2018JG002401](#), Sun, [10.1029/2018JG002401](#), eiluweit, [10.1029/2018JG002401](#), ang, [10.1029/2018JG002401](#), ang, [10.1029/2018JG002401](#), in, [10.1029/2018JG002401](#), ing, [10.1029/2018JG002401](#), 2019 Mobilization of ferric iron associated organic carbon during iron reduction: desorption versus coprecipitation [10.1029/2018JG002401](#), **0**, 61–68
- arris, [10.1029/2018JG002401](#), ones, [10.1029/2018JG002401](#), sborn, [10.1029/2018JG002401](#), ister, [10.1029/2018JG002401](#), 2014 Updated high-resolution grids of monthly climatic observations—the CRU TS3.10 dataset [10.1029/2018JG002401](#), **4**, 3, 623–642
- earth-sill Scallan, [10.1029/2018JG002401](#), Scatena, [10.1029/2018JG002401](#), strada, C, [10.1029/2018JG002401](#), c o ell, [10.1029/2018JG002401](#), ugo, [10.1029/2018JG002401](#), 2007 Disturbance and long-term patterns of rain fall and throughfall in

- trient fluxes in a subtropical wet forest in Puerto Rico. *Journal of Hydrology*, 333(2-4), 472-485.
- Henderson, R., Kabengi, N., Mantripragada, N., Cabrera, M., Hassan, S., & Thompson, A. (2012). Anoxia-induced release of colloid- and nanoparticle-bound phosphorus in grassland soils. *Environmental Science & Technology* 46(21), 11727-11734.
- Herndon, E., AlBashaireh, A., Singer, D., Chowdhury, T. R., Gu, B., & Graham, D. (2017). Influence of iron redox cycling on organo-mineral associations in arctic tundra soil. *Geochimica et Cosmochimica Acta* 207, 210-231.
- Herndon, E. M., Kinsman-Costello, L., Duroe, K. A., Mills, J., Kane, E. S., Sebestyen, S. D., ... Wulfschleger, S. D. (2019). Iron (oxyhydr)oxides serve as phosphate traps in tundra and boreal peat soils. *Journal of Geophysical Research: Biogeosciences* 124(2), 227-246.
- Hodges, C., Mallard, J., Markewitz, D., Barcellos, D., & Thompson, A. (2019). Seasonal and spatial variation in the potential for iron reduction in soils of the southeastern piedmont of the US. *Catena*, 180, 32-40.
- Hurrell, J. W., Holland, M. M., Gent, P. R., Ghan, S., Kay, J. E., Kushner, P. J., ... others (2013). The community earth system model: a framework for collaborative research. *Bulletin of the American Meteorological Society*, 94(9), 1339-1360.
- Jobbagy, E. G., & Jackson, R. B. (2000). The vertical distribution of soil organic carbon and its relation to climate and vegetation. *Ecological Applications*, 10(2), 423-436.
- Khan, I., Fahad, S., Wu, L., Zhou, W., Xu, P., Sun, Z., ... others (2019). Labile organic matter intensifies phosphorous mobilization in paddy soils by microbial iron (iii) reduction. *Geoderma* 352, 185-196.
- Kramer, M. G., & Chadwick, O. A. (2018). Climate-driven thresholds in reactive mineral retention of soil carbon at the global scale. *Nature Climate Change*, 8(12), 1104.
- LaCroix, R. E., Tfaily, M. M., McCreight, M., Jones, M. E., Spokas, L., & Keiluweit, M. (2019). Shifting mineral and redox controls on carbon cycling in seasonally flooded mineral soils. *Biogeosciences* 16(13), 2573-2589.
- Laio, F., Porporato, A., Ridol, L., & Rodriguez-Iturbe, I. (2001). Plants in water-controlled ecosystems: active role in hydrologic processes and response to water stress: II. probabilistic soil moisture dynamics. *Advances in Water Resources* 24(7), 707-723.
- LaRowe, D. E., & Van Cappellen, P. (2011). Degradation of natural organic matter: a thermodynamic analysis. *Geochimica et Cosmochimica Acta* 75(8), 2030-2042.
- Lovley, D. R. (1991). Dissimilatory Fe (iii) and Mn (iv) reduction. *Microbiological Reviews*, 55(2), 259-287.
- Malhi, Y., & Grace, J. (2000). Tropical forests and atmospheric carbon dioxide. *Trends in Ecology & Evolution*, 15(8), 332-337.
- Miller, A. J., Schuur, E. A., & Chadwick, O. A. (2001). Redox control of phosphorus pools in Hawaiian montane forest soils. *Geoderma* 102(3-4), 219-237.
- Morel, F. M., Hering, J. G., et al. (1993). Principles and applications of aquatic chemistry. John Wiley & Sons.
- Oertel, C., Matschullat, J., Zuerba, K., Zimmermann, F., & Erasmí, S. (2016). Greenhouse gas emissions from soils: a review. *Chemie der Erde-Geochemistry* 76(3), 327-352.
- Richter, D. D., & Markewitz, D. (2001). Understanding soil change. *Understanding Soil Change*, by Daniel D. Richter, Jr and Daniel Markewitz and Foreword by William A. Reinert and Pedro Sanchez, pp. 272. ISBN 0521771714. Cambridge, UK: Cambridge University Press, June 2001, 1.
- Roden, E. E., & Wetzel, R. G. (1996). Organic carbon oxidation and suppression of

- methane production by microbial Fe (iii) oxide reduction in vegetated and un-vegetated freshwater wetland sediments. *Limnology and Oceanography* 41(8), 1733{1748.
- Rout, G. R., & Sahoo, S. (2015). Role of iron in plant growth and metabolism. *Reviews in Agricultural Science*, 3, 1{24.
- Scatena, F. N. (1989). An introduction to the physiography and history of the bisley experimental watersheds in the Luquillo mountains of Puerto Rico. Gen. Tech. Rep. SO-72. New Orleans, LA: US Dept of Agriculture, Forest Service, Southern Forest Experiment Station. 22 p, 72.
- Stucki, J. W. (2011). A review of the effects of iron redox cycles on smectite properties. *Comptes Rendus Geosciences* 343(2-3), 199{209.
- Thompson, A., Chadwick, O. A., Rancourt, D. G., & Chorover, J. (2006). Iron-oxide crystallinity increases during soil redox oscillations. *Geochimica et Cosmochimica Acta*, 70(7), 1710{1727.
- Todd-Brown, K. E., Hopkins, F. M., Kivlin, S. N., Talbot, J. M., & Allison, S. D. (2012). A framework for representing microbial decomposition in coupled climate models. *Biogeochemistry*, 109(1-3), 19{33.
- Vermeire, M.-L., Bonneville, S., Stenuit, B., Delvaux, B., & Correlis, J.-T. (2019). Is microbial reduction of Fe (iii) in podzolic soils influencing C release? *Geoderma*, 340, 1{10.
- Vogel, R., & Sankarasubramanian, A. (2005). Monthly climate data for selected USGS HCDN sites, 1951-1990, r1. ORNL Distributed Active Archive Center. Retrieved from [http://daac.ornl.gov/cgi-bin/dsviewer.pl?ds\\_id=810](http://daac.ornl.gov/cgi-bin/dsviewer.pl?ds_id=810) doi: 10.3334/ORNLDAAAC/810
- Wang, Y., Liu, C., Peng, A., & Gu, C. (2019). Formation of hydroxylated polychlorinated diphenyl ethers mediated by structural Fe (iii) in smectites. *Chemosphere*, 226, 94{102.
- Weiss, J. V., Emerson, D., & Megonigal, J. P. (2004). Geochemical control of microbial Fe (iii) reduction potential in wetlands: comparison of the rhizosphere to non-rhizosphere soil. *FEMS Microbiology Ecology*, 48(1), 89{100.
- Weiss, J. V., Emerson, D., & Megonigal, J. P. (2005). Rhizosphere iron (iii) deposition and reduction in a l.-dominated wetland. *Soil Science Society of America Journal*, 69(6), 1861{1870.
- Yang, W. H., & Liptzin, D. (2015). High potential for iron reduction in upland soils. *Ecology*, 96(7).
- Yu, H.-Y., Li, F.-B., Liu, C.-S., Huang, W., Liu, T.-X., & Yu, W.-M. (2016). Iron redox cycling coupled to transformation and immobilization of heavy metals: implications for paddy rice safety in the red soil of south China. In *Advances in agronomy* (Vol. 137, pp. 279{317). Elsevier.
- Zheng, J., Thornton, P. E., Painter, S. L., Gu, B., Wulfschleger, S. D., & Graham, D. E. (2019). Modeling anaerobic soil organic carbon decomposition in arctic polygon tundra: insights into soil geochemical influences on carbon mineralization. *Biogeosciences* 16(3), 663{680.